Supplementary Material and Methods:

PNPLA1 Deficiency in Mice and Humans Leads to a Defect in the Synthesis of Omega-O-acylceramides

Susanne Grond[1], Thomas O. Eichmann[1], Sandrine Dubrac[2], Dagmar Kolb[3,4,5], Matthias Schmuth[2], Judith Fischer[6], Debra Crumrine[7], Peter M. Elias[7], Guenter Haemmerle[1], Rudolf Zechner[1], Achim Lass[1], and Franz P.W. Radner[1]

[1] Institute of Molecular Biosciences, University of Graz, Graz, Austria; [2] Department of Dermatology, Venerology, and Allergology, Innsbruck Medical University, Innsbruck, Austria; [3] ZMF, Center for Medical Research, Medical University of Graz, Graz, Austria; [4] Institute of Cell Biology, Histology, and Embryology, Medical University of Graz, Graz, Austria; [5] BioTechMed-Graz, Graz, Austria; [6] Institute for Human Genetics, University Medical Center Freiburg, Freiburg i. Br., Germany; and [7] Dermatology Service, Department of Veterans Affairs Medical Center, University of California, San Francisco, California, USA.

Correspondence: Franz P.W. Radner, Institute of Molecular Biosciences, University of Graz, Graz, Austria. E-mail: franz.radner@uni-graz.at

SUPPLEMENTARY TABLES AND FIGURES

Table S1. Comparison of body weight and length of newborn wild-type, *Pnpla1*$^{+/-}$, and *Pnpla1*$^{-/-}$ mice.

	wild-type		***Pnpla1*$^{+/-}$**		***Pnpla1*$^{-/-}$**	
	wet	dry	wet	dry	wet	dry
weight [mg]	1,393.3 ± 72.40	226.9 ± 13.54	1,392.5 ± 85.19	227.2 ± 17.76	1,069.2 ± 74.77[a]	179.5 ± 11.56[a]
length [mm]	37.3 ± 1.15	24.8 ± 0.75	37.5 ± 0.80	24.5 ± 0.52	32.4 ± 0.90[a]	21.7 ± 0.65[a]

All parameters were measured before and after drying of mice at 60 °C. Data are presented as means ± SD (n = 12 mice/genotype). [a] Effect of genotype; statistically significant differences were determined by unpaired two-tailed Student's *t*-test ($P < 0.001$) in comparison to wild-type mice. PNPLA1, patatin-like phospholipase domain-containing 1.

Table S2. Comparison of blood parameters in newborn wild-type, *Pnpla1*$^{+/-}$, and *Pnpla1*$^{-/-}$ mice.

	wild-type		***Pnpla1*$^{+/-}$**		***Pnpla1*$^{-/-}$**	
postpartum	~ 1 hour	~ 8−10 hours	~ 1 hour	~ 8−10 hours	~ 1 hour	~ 8−10 hours
FA [mmol/liter]	0.035 ± 0.083	0.60 ± 0.092[a]	0.035 ± 0.074	0.60 ± 0.061[a]	0.023 ± 0.059	0.023 ± 0.07[b]
TAG [mg/deciliter]	39.2 ± 12.59	80.7 ± 22.00[a]	39.7 ± 8.65	81.6 ± 15.29[a]	29.2 ± 2.84	30.1 ± 7.35[b]
glucose [mg/deciliter]	37.9 ± 9.01	72.4 ± 11.35[a]	40.4 ± 10.74	72.5 ± 11.69[a]	33.3 ± 11.32	36.1 ± 6.13[b]

All parameters were measured ~ 1 hour (before first suckling) or ~ 8−10 hours postpartum. Data are presented as means ± SD (n = 6−8 mice/genotype and group). [a] Effect of suckling; statistically significant differences between 1 hour and 8−10 hours postpartum measurements of the same genotype were determined by unpaired two-tailed Student's *t*-test ($P < 0.001$). [b] Effect of genotype; statistically significant differences were determined by unpaired two-tailed Student's *t*-test ($P < 0.001$) in comparison to wild-type mice. FA, fatty acid; PNPLA1, patatin-like phospholipase domain-containing 1; TAG, triacylglycerol.

Table S3. Primer pairs used for mRNA expression analysis of target genes by quantitative real-time reverse transcriptase-PCR (qRT-PCR).

primer name	sequence
***Actb* forward**	5'-AGC CAT GTA CGT AGC CAT CCA-3'
***Actb* reverse**	5'-TCT CCG GAG TCC ATC ACA ATG-3'
***Aloxe3* forward**	5'-ATG GCA GTA TAT CGG CTG TGT-3'
***Aloxe3* reverse**	5'-GCT TCT GCT TAG GGC TTT CAC-3'
***Alox12b* forward**	5'-GGG GAC GCT GGA TTC AAT TTC-3'
***Alox12b* reverse**	5'-GGC ACT GTA CCG TGT AGT CAT-3'
***Asah1* forward**	5'-TCC GTG GCA CAC CAT AAA TCT-3'
***Asah1* reverse**	5'-TCC ACT TGG CAC AAA TGT ATT CA-3'
***Gba* forward**	5'-GCC AGG CTC ATC GGA TTC TTC-3'
***Gba* reverse**	5'-CAC GGG GTC AAG AGA GTC AC-3'
***Pnpla1* forward**	5'-TCT TCC ATG ACT TCC GAA TG-3'
***Pnpla1* reverse**	5'-CCT GCA GAA TCA CCA GGT C-3'
***Rplp0* forward**	5'-GCT TCA TTG TGG GAG CAG ACA-3'
***Rplp0* reverse**	5'-CAT GGT GTT CTT GCC CAT CAG-3'
***Tgm1* forward**	5'-AAC CGG GAA TAT GAG TCC TCT G-3'
***Tgm1* reverse**	5'-CGT TGT TCT TAG TCA CTT GGG C-3'

ACTB, actin beta; ALOXE3, arachidonate lipoxygenase 3; ALOX12B, arachidonate 12-lipoxygenase, 12R type; ASAH1, N-acylsphingosine amidohydrolase 1; GBA, glucosylceramidase beta; PNPLA1, patatin-like phospholipase domain-containing 1; RPLP0, ribosomal protein lateral stalk subunit P0; TGM1, transglutaminase 1.

Table S4. Primary antibodies used for immunoblot analyses.

antibody	source
anti-β-actin	# sc-47778, Santa Cruz Biotechnology, Dallas, TX
anti-FABP5	# AF1476, R&D Systems, Minneapolis, MN
anti-filaggrin	# PRB-417P, BioLegend, San Diego, CA
anti-involucrin	# PRB-140P, BioLegend, San Diego, CA
anti-loricrin	# PRB-145P, BioLegend, San Diego, CA
anti-PNPLA1	self-made antibody raised against a synthetic peptide corresponding to amino acid residues 379−395 of murine PNPLA1

FABP5, fatty acid binding protein 5; PNPLA1, patatin-like phospholipase domain-containing 1.

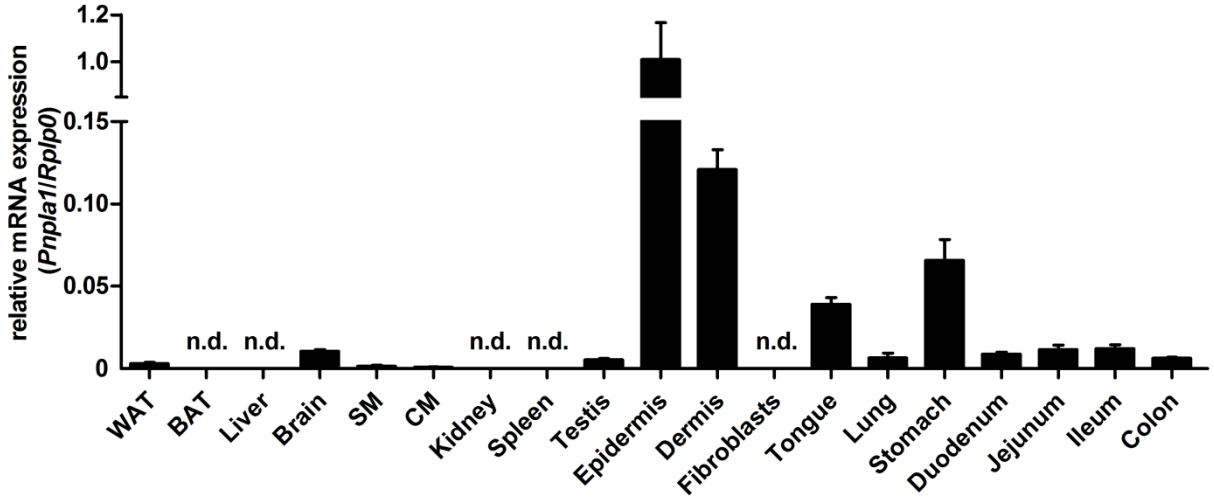

Figure S1. Tissue-specific expression of *Pnpla1* in mice. Relative *Pnpla1* mRNA expression level in different tissues and isolated dermal primary fibroblasts from adult C57BL/6J mice analyzed by qRT-PCR. Data are presented as means + SD (n = 3 mice or independent culture dishes). C/SM, cardiac/skeletal muscle; n.d.; not detectable; PNPLA1, patatin-like phospholipase domain-containing 1, qRT-PCR, quantitative real-time reverse transcriptase-PCR; RPLP0, ribosomal protein lateral stalk subunit P0; W/BAT, white/brown adipose tissue.

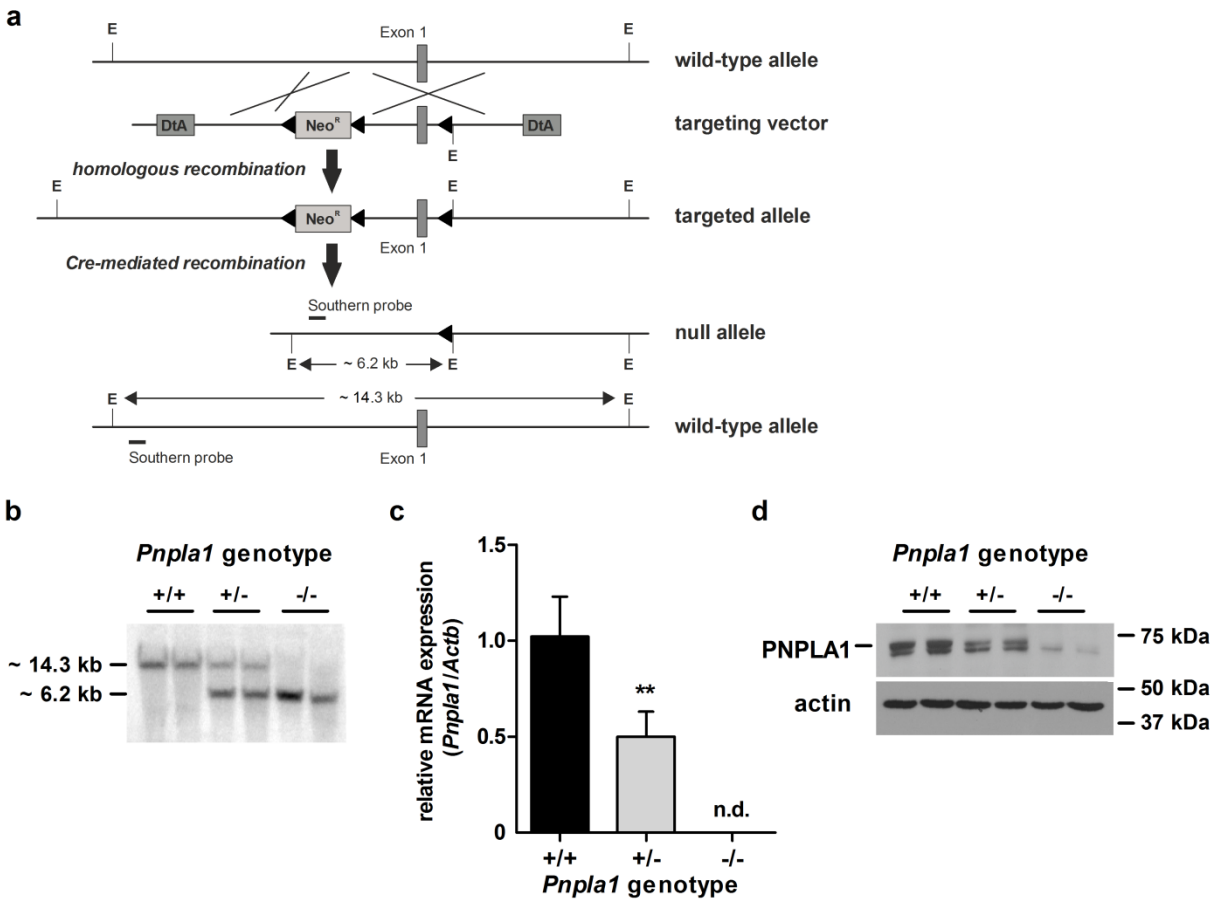

Figure S2. Generation of PNPLA1-deficient mice. (**a**) Homologous recombination of the targeting vector with the *Pnpla1* wild-type allele introduced a *lox*P site (◄) in intron 1 and a neomycin resistance gene cassette (Neo^R) flanked by *lox*P sites into the upstream sequence of exon 1. Cre recombinase-mediated recombination resulted in deletion of the neomycin resistance gene cassette and *Pnpla1* exon 1. The targeted allele was identified by EcoRV (E) restriction digest. In silico hybridization with a Southern probe (solid bar) gave a 14.3 and 6.2 kb DNA fragment for the wild-type and null allele, respectively. (**b**) Analysis of EcoRV-digested genomic DNA from newborn mice by Southern blotting using a probe specific for the upstream region of the *Pnpla1* gene. Autoradiography signals obtained from DNA fragments of 14.3 and 6.2 kb corresponded to wild-type (+) and targeted *Pnpla1* (−) alleles, respectively. (**c**) Relative epidermal *Pnpla1* mRNA expression level analyzed by qRT-PCR. Data are presented as means + SD (n = 4 mice/genotype). Statistically significant differences were determined by unpaired two-tailed Student's *t*-test (**$P < 0.01$). (**d**) Immunoblot analysis of PNPLA1 protein expression levels in epidermal lysates using a rabbit anti-PNPLA1 antiserum and actin as loading control. ACTB, actin beta; n.d., not detectable; PNPLA1, patatin-like phospholipase domain-containing 1; qRT-PCR, quantitative real-time reverse transcriptase-PCR.

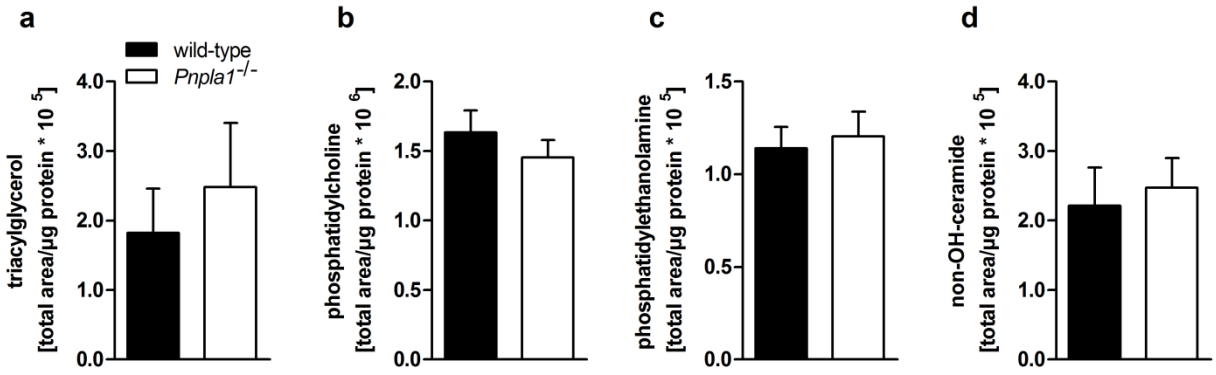

Figure S3. Unchanged levels of neutral and polar lipids as well as non-OH-ceramides in PNPLA1-deficient skin. Epidermal (**a**) triacylglycerol, (**b**) phosphatidylcholine, (**c**) phosphatidylethanolamine, and (**d**) non-OH-ceramide content quantified by UPLC-qTOF analyses in lipid extracts from newborn wild-type and *Pnpla1*$^{-/-}$ mice. Peak areas of lipid species were combined and normalized to epidermal protein content. Data are presented as means + SD (n = 3−4 mice/genotype) and representative for two independent experiments. PNPLA1, patatin-like phospholipase domain-containing 1; UPLC-qTOF, ultra-performance liquid chromatography-quadrupole time of flight.

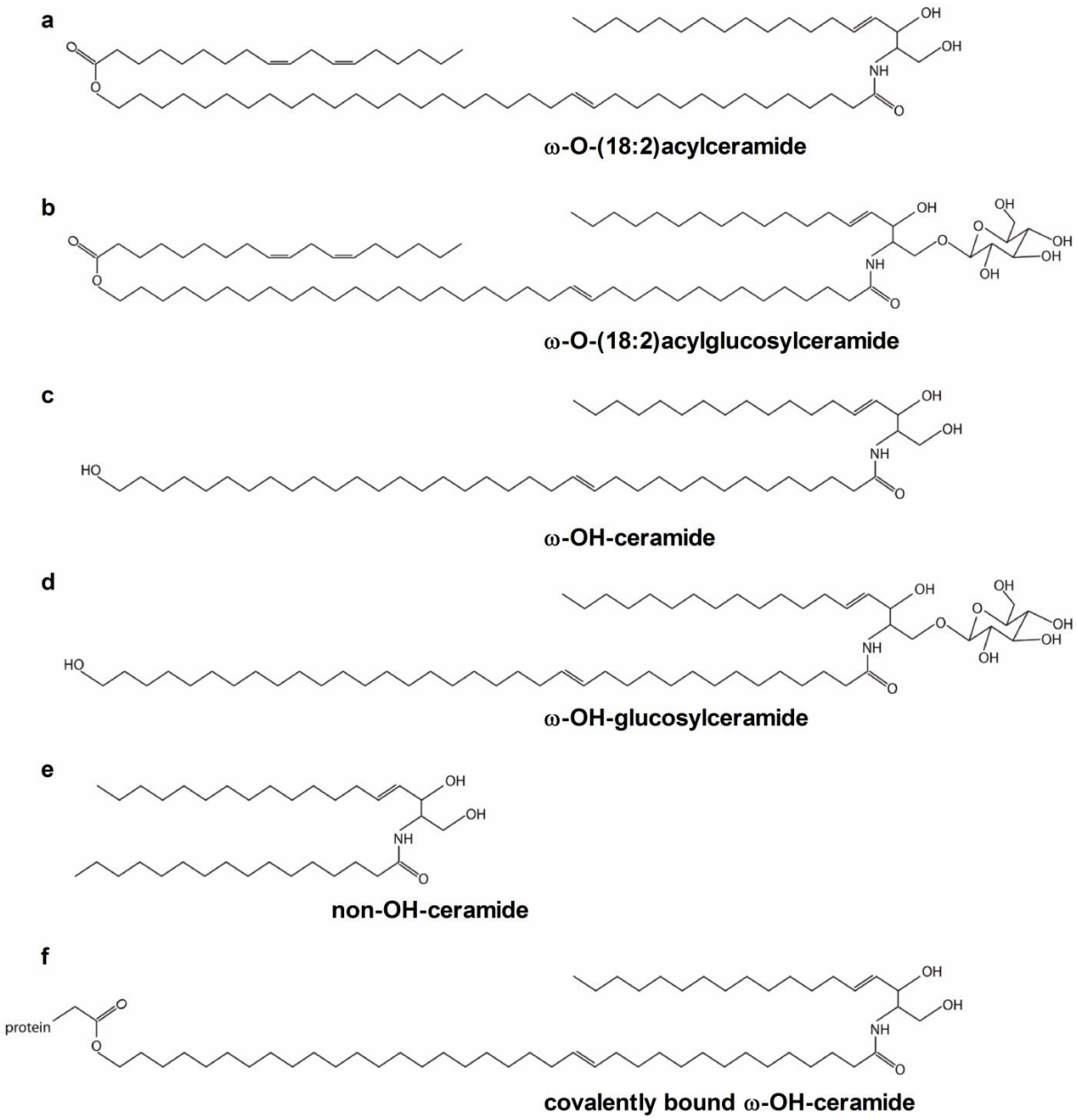

Figure S4. Molecular structure of ceramide classes analyzed in this study.

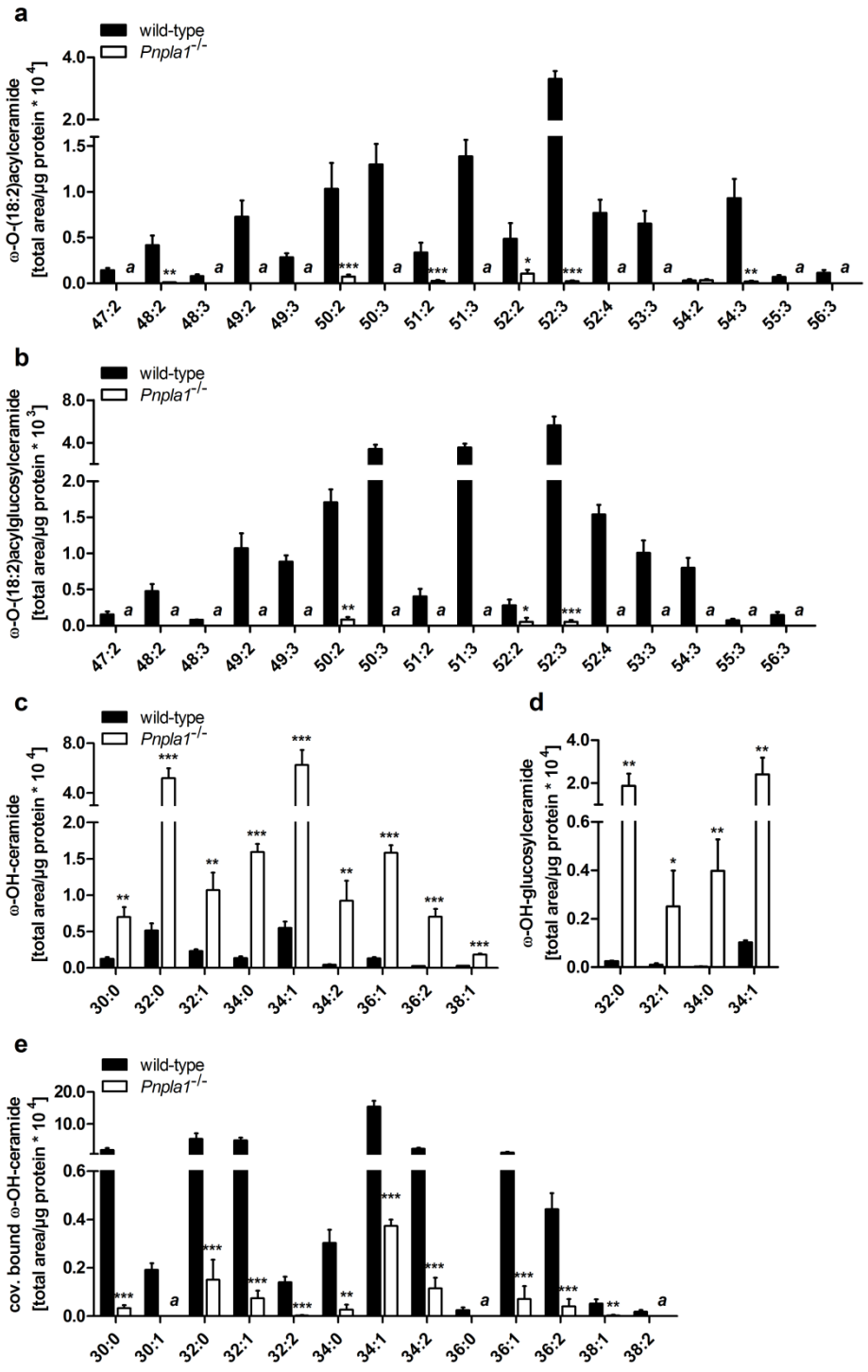

Figure S5. Lack of ω-O-acylceramides in PNPLA1-deficient skin. Content of epidermal (**a**) ω-O-(18:2)acylceramide, (**b**) ω-O-(18:2)acylglucosylceramide, (**c**) ω-OH-ceramide, (**d**) ω-OH-glucosylceramide, and (**e**) covalently bound ω-OH-ceramide species quantified by UPLC-qTOF analyses in lipid extracts from newborn wild-type and *Pnpla1*$^{-/-}$ mice. Peak areas of lipid species were normalized to epidermal protein content. Data are presented as means + SD (n = 3−4 mice/genotype) and representative for two independent experiments. Statistically significant differences were determined by unpaired two-tailed Student's *t*-test (**P* < 0.05, ***P* < 0.01, ****P* < 0.001) between genotypes. [a] Lipid content of ceramide species below limit of quantification. PNPLA1, patatin-like phospholipase domain-containing 1; UPLC-qTOF, ultra-performance liquid chromatography-quadrupole time of flight.

SUPPLEMENTARY METHODS

Generation of PNPLA1-deficient mice

For the generation of the *Pnpla1* gene targeting vector, a 2.0 kb sized DNA fragment encompassing *Pnpla1* exon 1 genomic sequence was amplified by PCR from genomic murine HM-1 embryonic stem cell DNA using Phusion® High-Fidelity DNA Polymerase (Finnzymes, Espoo, Finland) and the forward primer 5'-GGA CTA GTT GAG GAC CGG TGT TCA GTT C-3' and reverse primer 5'-AGG AAT TCC CAC ATC TGT CAC CAG CTT CTC-3'. The PCR product was digested with SpeI and EcoRI restriction enzymes and ligated into the pBlueScript II KS (-) vector (Stratagene, La Jolla, CA) downstream of a *lox*P recombination site. Next, a 2.0 kb DNA fragment upstream of *Pnpla1* exon 1 was amplified by PCR using the forward primer 5'-GAG CGG CCG CGA GCT GTC TTT CTA CCT CCT AAA TC-3' and the reverse primer 5'-GCT CTA GAC CGT GCA GGT CTT CTC TCT TG-3'. After a NotI-XbaI digest, the PCR product was cloned into a pBK-CMV plasmid harboring a neomycin resistance gene cassette flanked by *lox*P sites. Subsequently, the resulting plasmid was digested with NotI and SpeI and the obtained 3.3 kb DNA fragment was ligated into the plasmid harboring the insertion of the *Pnpla1* exon 1 genomic sequence and the *lox*P recombination site. Finally, a 1.9 kb sized DNA fragment downstream of *Pnpla1* exon 1 was amplified by PCR using the forward primer 5'-TTG ATA TCG GAC ACA GTG TGG GAG CTT C-3' and the reverse primer 5'-ATC AAG CTT CCT GGC TAA CCT GGA ATT CAC-3', and ligated into the pBlueScript II KS (-) vector using EcoRV and HindIII. After an EcoRV-ClaI restriction digest, the resulting fragment was ligated into the pBlueScript II KS (-) plasmid downstream of the single *lox*P site and next to the *Pnpla1* exon1 genomic sequence. From the resulting plasmid, a 7.2 kb DNA fragment, encompassing the gene targeting construct, was released by restriction digest with NotI and ClaI, and ligated into a pUC plasmid harboring two DtA gene cassettes.

The vector was linearized by restriction digest with ScaI and introduced into HM-1 embryonic stem cells by electroporation. Geniticin-resistant clones were picked and expanded. (G418 was purchased from Invitrogen Life Technologies, Carlsbad, CA). Cell clones that underwent homologous recombination were identified by PCR. Embryonic stem cell clones heterozygous for the targeted *Pnpla1* allele were injected into 3.5 days old C57BL/6J host blastocysts and transferred into the uterine horn of (C57BL/6J×CBA/J) F1 pseudo pregnant foster mothers to generate chimeras. To obtain mice harboring a *Pnpla1* null allele, male chimeric mice exhibiting a coat color chimerism greater than 70% were bred with mice expressing Cre-recombinase driven by the human cytomegalovirus (CMV) minimal promoter that led to deletion of *lox*P-flanked sequences in all tissues and cell types, including germ cells. Germline transmission of the targeted allele was verified by coat color pigmentation and confirmed by Southern blot analysis. Heterozygous mice for the targeted *Pnpla1* allele were backcrossed at least 5 times with C57BL/6J mice (i.e. 98.4% C57BL/6J background) prior to any further analysis.

Southern blot analysis and genotyping

Analysis of genomic DNA was performed as described previously (Radner et al. 2010). The external probe for DNA analysis was generated by PCR from HM-1 genomic ES cell DNA using the forward primer 5'-AGG AAT TCT TGG TTG GGT ATT GAG GGA C-3' and the reverse primer 5'-AGG AAT TCA CCC TCT TCT CTT TCA CTC TGC-3', and cloned into the pBlueScript II KS (-) vector using EcoRI.

Genotyping of mice was routinely performed by PCR analysis of tail tip DNA using FIREPol® DNA polymerase (Solis BioDyne, Tartu, Estonia) and the following primers in a single reaction: forward I: 5'-CTG CCT TAG TGA TCC GCA GT-3'; forward II: 5'-CAA CTT CCC AGT GAG GAG GA-3'; reverse: 5'-TAC ATT ACA GCC TGG CAT CG-3'.

Skin histology and ultrastructural analysis

Biopsies from mouse dorsal skin were fixed in 4% formaldehyde, paraffin embedded, sectioned, and stained with hematoxylin and eosin. For transmission electron microscopy, biopsies from mouse dorsal skin were fixed in 2.5% glutaraldehyde and 2.0% paraformaldehyde in 0.1 M cacodylate buffer, pH 7.4, post-fixed in 2.0% osmium tetroxide in 0.2 M cacodylate buffer, dehydrated, and embedded in TAAB epoxy resin (TAAB Agar Scientific, Essex, UK). 70-nm-thick sections were contrasted with 3% uranyl acetate and 2.5% lead citrate, and examined using an FEI Tecnai G2 20 transmission electron microscope (FEI, Eindhoven, The Netherlands) equipped with a Gatan ultrascan 1000 ccd camera. For analysis of the corneocyte-bound lipid envelope by transmission electron microscopy, frozen biopsies from mouse dorsal skin were thawed in pyridine for 2 hours and then fixed in 2.0% glutaraldehyde and 2.0% paraformaldehyde in 0.1 M cacodylate buffer overnight. Tissues were then rinsed and post-fixed in 1.0% osmium tetroxide in 0.2 M cacodylate buffer for 1 hour, dehydrated through a grades series of alcohol, followed by two changes of propylene oxide, and embedded in epoxy resin. The samples were cut on a Leica Ultracut E microtome (Leica microsystems, Wetzlar, Germany) and imaged on a JEOL 100CX transmission electron microscope (JEOL, Tokyo, Japan) using a Gatan digital camera.

Epidermal lipid analysis

Epidermal lipids were extracted three times with chloroform/methanol/ glacial acetic acid (66/33/1, v/v/v) containing 4 nmol N-heptadecanoyl-D-*erythro*-sphingosine (C17 ceramide, Avanti Polar Lipids, Alabaster, AL) per sample as internal standard. Phase separation was obtained by the addition of 1/5 volume of water and centrifugation at 1,400 x g for 10 minutes at room temperature. The lower organic phase containing the lipids was collected and dried under a stream of nitrogen. Remaining epidermal sheets were solubilized in 0.3 N NaOH at 65°C overnight and the protein content was determined using Pierce™ BCA reagent (Thermo Fisher Scientific, Waltham, MA) and BSA as standard. For extraction of covalently bound epidermal lipids, alkaline-hydrolyzed samples were extracted with chloroform/methanol/glacial acetic acid (66/33/1, v/v/v) including C17 ceramide as internal standard. After phase separation, the lower organic phase was collected and dried as described above.

For ultra-performance liquid chromatography-quadrupole time of flight (UPLC-qTOF) analysis of neutral and polar epidermal lipids, dried lipid extracts were dissolved in chloroform/methanol/2-propanol (2/1/12, v/v/v). Chromatographic separation was performed using

an AQUITY-UPLC system (Waters Corporation, Milford, MA), equipped with a HSS T3 column (2.1x100 mm, 1.8µm; Waters Corporation) as described (Knittelfelder et al. 2014). A SYNAPT™G1 qTOF HD mass spectrometer (Waters Corporation) equipped with an ESI source was used for detection. Data acquisition was done by the MassLynx 4.1 software (Waters Corporation). Lipid classes were analyzed with the "Lipid Data Analyzer 1.6.2" software (Hartler et al. 2011). Extraction efficacy and lipid recovery was verified using the internal standard. A response correction was not performed for any analyzed lipid species.

Measurement of in vivo ω-O-acylceramide synthesis in human primary keratinocytes and murine epidermal explants

Human primary keratinocytes were cultivated and in vitro differentiated for 14 days as described (Radner et al. 2013). For analysis of in vivo ω-O-acylceramide synthesis, keratinocyte cultures on day 13 of differentiation or dorsal 3 x 3-mm sized epidermal explants were incubated in EpiLife medium (Invitrogen Life Technologies) containing 1.1 mM $CaCl_2$, 30 µM palmitic acid, and 20 µM [1-^{14}C] linoleic acid (55 mCi/mmmol; GE Healthcare, Buckinghamshire, UK) complexed to essentially fatty acid (FA) free BSA at a molar FA/BSA ratio of 3:1. After 24 hours at 37 °C, epidermal explants and keratinocyte cultures were washed with PBS and epidermal lipids were extracted as described above, dried, reconstituted in chloroform, and spotted onto a thin-layer Silica Gel 60 plate (Merck, Summit, NJ). Epidermal ceramide species were separated twice using chloroform/methanol/acetic acid (190/9/1, v/v/v) as solvent system and N-(30-linoleoyloxy-triacontanoyl)-sphingosine (ω-O-acylceramide, Matreya LLC, State College, PA) as internal standard. Autoradiography signals were obtained by exposure of developed plates to PhosphorImager screens (GE Healthcare) and analyzed by a Storm scanner (GE Healthcare). Levels of brightness, saturation, and contrast were optimized for low signal intensities prior to image generation and output using Storm-associated software. Subsequently, separated lipids were visualized by iodine vapor or by charring, and radioactivity in lipid bands co-migrating with the ω-O-acylceramide standard was determined by liquid scintillation counting.

In vivo transfer of murine skin lipids

Epidermal ceramide species were ex vivo radiolabeled by incubation of epidermal explants in EpiLife Medium containing 1.1 mM $CaCl_2$, 60 µM linoleic acid, and 90 µM [1-^{14}C] palmitic acid (55 mCi/mmol; Hartmann Analytics GmbH, Braunschweig, Germany) complexed to essentially FA free BSA at a molar FA/BSA ratio of 3:1. Lipids were extracted as described above, dried, and reconstituted in 1,2-propanediol/2-propanol (7/3, v/v) (Zettersten et al. 1997). Ten µl of radiolabeled lipid extract (5 x 10^5 cpm/µl) were applied onto an approximately 10 x 7 mm² skin area of *Pnpla1*-mutant mice immediately after birth. Mice were then placed at 30 °C and 80% humidity. After 6 hours, covalently bound lipids were isolated and analyzed by thin-layer chromatography as described above using N-ω-hydroxytriacontanoyl-D-*erythro*-sphingosine (ω-hydroxy-ceramide, Matreya LLC) and oleic acid (Sigma-Aldrich, St. Louis, MO) as internal standards. Autoradiography signals and radioactivity contained in lipid bands co-migrating with the ω-hydroxy-ceramide standard were determined as described above.

SUPPLEMENTARY REFERENCES

Hartler J, Trötzmüller M, Chitraju C, Spener F, Köfeler HC, Thallinger GG. Lipid Data Analyzer: unattended identification and quantitation of lipids in LC-MS data. Bioinformatics. 2011;27:572–7.

Knittelfelder OL, Weberhofer BP, Eichmann TO, Kohlwein SD, Rechberger GN. A versatile ultra-high performance LC-MS method for lipid profiling. J Chromatogr B. 2014;951-952:119–28.

Radner FP, Marrakchi S, Kirchmeier P, Kim G-J, Ribierre F, Kamoun B, et al. Mutations in CERS3 cause autosomal recessive congenital ichthyosis in humans. PLoS Genet. 2013;9:e1003536.

Radner FP, Streith IE, Schoiswohl G, Schweiger M, Kumari M, Eichmann TO, et al. Growth retardation, impaired triacylglycerol catabolism, hepatic steatosis, and lethal skin barrier defect in mice lacking comparative gene identification-58 (CGI-58). J Biol Chem. 2010;285:7300–11.

Zettersten EM, Ghadially R, Feingold KR, Elias PM, Francisco S. Optimal ratios of topical stratum corneum lipids improve barrier recovery in chronologically aged skin. J Am Acad Dermatol. 1997;37:403–8.